J Therm Spray Tech (2024) 33:771–785
https://doi.org/10.1007/s11666-024-01742-2

ORIGINAL RESEARCH ARTICLE

Copper Coatings for Antibiotics Reduction in Fattening Livestock

Lukas Möhrke[1] · Michél Hauer[1] · Andreas Gericke[1] · Anne Breitrück[2] · Bernd Kreikemeyer[3] · Knuth-Michael Henkel[4]

Submitted: 15 June 2023 / in revised form: 30 January 2024 / Accepted: 30 January 2024 / Published online: 28 February 2024

Abstract In the current work, twin-wire arc-sprayed copper coatings are investigated to reduce the spread of pathogenic germs in broiler farming. Compressed air and nitrogen are used as process gasses, while the coating torches are varied. The results demonstrate a reduction of 99% pathogenic load due to the presence of coatings in comparison with the uncoated nickel-chromium-steel. This accounts especially for the bacterial strains *E.coli, S.aureus and E.cecorum*, which are the predominant bacteria in broiler farming. Moreover, posttreatment processes like cold plasma, tungsten inert gas arc processing and shot peening are investigated to further increase the bactericidal properties and abrasion resistance characteristics of the coatings. Further investigations involve the microstructure and the electrical conductivity of the coatings. In this work, it is demonstrated that copper-coated surfaces have an inhibitory effect on bacterial growth of the three investigated bacterial strains compared to the uncoated bulk nickel-chromium-steel material.

Keywords abrasive wear · antibiotic reduction · antipathogenic coating · nitrogen · wire arc spray

This article is an invited paper selected from presentations at the 2023 International Thermal Spray Conference, held May 22–25, 2023, in Québec City, Canada, and has been expanded from the original presentation. The issue was organized by Giovanni Bolelli, University of Modena and Reggio Emilia (Lead Editor); Emine Bakan, Forschungszentrum Jülich GmbH; Partha Pratim Bandyopadhyay, Indian Institute of Technology, Karaghpur; Šárka Houdková, University of West Bohemia; Yuji Ichikawa, Tohoku University; Heli Koivuluoto, Tampere University; Yuk-Chiu Lau, General Electric Power (Retired); Hua Li, Ningbo Institute of Materials Technology and Engineering, CAS; Dheepa Srinivasan, Pratt and Whitney; and Filofteia-Laura Toma, Fraunhofer Institute for Material and Beam Technology.

✉ Lukas Möhrke
lukas.moehrke@igp.fraunhofer.de

[1] Thermal Joining Engineering, Fraunhofer Institute for Large Structures in Production Engineering IGP, Rostock, Germany

[2] Extracorporeal Immunomodulation, Fraunhofer Institute for Cell Therapy and Immunology IZI, Rostock, Germany

[3] Institute of Medical Microbiology, Virology and Hygiene, Chair of Molecular Bacteriology, University Medicine Rostock UMR, Rostock, Germany

[4] Chair of Joining Technology, University of Rostock, Rostock, Germany

Introduction

Currently, there is no experience in producing antipathogenic surfaces in broiler farming. Instead, current drinking nipples for the livestock are made up of nickel-chromium-steel alloys, which are not resistant against viruses, bacteria and fungi (Ref 1, 2). This type of drinking system is used in almost 90% of broiler houses (Ref 3).

As a result, the use of antibiotics in broiler farming is increasing, leading to the spread of antibiotic-resistant pathogens in the food industry (Ref 4). This poses a serious health risk for humans and animals (Ref 4). Therefore, several metal coatings (Cu, Ag-alloys) applied by thermal spraying are becoming the focus of attention due to their high antipathogenic effect and resistance against abrasion (Ref 5, 6).

The potential of copper to promote antiseptic and health effects has been known for thousands of years. Over the years, the number of publications and patent applications related to antiseptic properties of copper have steadily increased (Ref 7, 8). With the growing market for antimicrobial coatings in healthcare, copper offers the highest

probability of success for antimicrobial activity (Ref 9, 10). In addition, recent research by the US Environmental Protection Agency (EPA) showed that Cu surfaces can kill 99.9% of disease-causing bacteria in a two-hour period when cleaned regularly (Ref 11, 12). Furthermore, a comparative study has shown that thermally sprayed copper coatings have antibacterial properties (Ref 13). Therefore, twin-wire arc spraying is chosen as coating process for the current work. Cost effectiveness as well as excellent deposition rates are the advantages of this thermal spray process (Ref 9). Preliminary own test results demonstrated that arc-sprayed copper surfaces reduced the pathogen load significantly. Thus, in the current work, a 99% copper alloy is arc-sprayed considering its antipathogenic effects, easy process handling and customizable coating properties. Additionally, the literature reveals that posttreatment by a plasma electric arc can increase the effectiveness of the coatings because of surface enlargement, cleaning and electrochemical activation (Ref 14).Thus, plasma posttreatment is used to increase the antipathogenic effectivity of the copper-based coatings. Moreover, posttreatment method with cold plasma demonstrates a reduction in bacterial growth. The interaction between cold plasma and materials is already known from biomedical engineering and is used here, to adapt the surface properties of biomaterials (Ref 15, 16).

Further investigations consist of the microstructure, the electrical conductivity and the abrasion behavior of the coatings. In order to be able to examine the wear resistance of the copper coatings, a wear test rig according to ASTM G65 is constructed (Ref 17). In addition, options were found to increase the abrasion resistance. Posttreatment methods, such as sandblasting with spherical blasting agents, shows a potential of increasing the strength of the coatings (Ref 18, 19).

Experimental Methods

The following flow diagram in Fig. 1 illustrates the process chain of the investigations carried out.

Spray Process and Materials

Arc spraying experiments were performed by using a GTV Sparc400 power source. (GTV Verschleißschutz GmbH, Luckenbach, DEU). The wires used were of type GTV CU99 (GTV Verschleißschutz GmbH, Luckenbach, DEU), which corresponds to a composition of 99% Cu. Two different series of experiments were performed. For the first series (V1.1 and V1.2) the torch Shark1000 was used, with compressed air and nitrogen as process gas. To avoid the burning off copper as well as oxidation of the particles under high-temperature nitrogen was selected as the process gas. The substrates used for the first series were Al alloy substrates with dimensions of approximately $10 \times 10 \times 6$ mm^3. This series consisted of preliminary tests of already sprayed copper coatings. The antipathogenic properties of these copper coatings were to be essentially proven. In the second series (V2.1-V2.4) the Shark 400RE and the Shark400HV torches were compared. The substrates of the second series consisted of hot rolled steels of type 1.4301 with the dimensions of approx. $58 \times 50 \times 8$ mm^3. The aim of this series was to specifically increase the coating quality and to compare different stainless steel drinking nipples used in fattening livestock husbandry.

Prior to spraying, the substrates were grit-blasted using corundum (size F24) and finally cleaned with isopropyl alcohol. The varying parameters and desired thicknesses can be found in Tables 1 and 2 along with the produced coating thickness and the deposition efficiency (DE). While the DE was specified following ISO 17836, the coating thickness was determined in cross-sections following the procedure described. hereafter, in "Microstructure". The experimental setup consisted of a firmly clamped substrate and a six-axis robot on which the twin-wire arc spray gun was mounted. During the test, the robot was operated in a linear spray pattern. Moreover, the constant spray parameter including the kinematics of the experiments for the series 1 and 2 can be found in Tables 3 and 4, respectively. From here on, the materials shall be referred using the abbreviations mentioned in the tables.

Microstructure

For microstructural analysis, the specimens were first cold mounted (two-phase system: liquid hardener and powder resin) and gradually grinded and polished (6, 3 µm and finally oxide polished). Coating thickness was determined by using an optical microscope (OM) Leica DM6000M (Leica Microsystems GmbH, Wetzlar, Germany) and the software tool "dhs-Bilddatenbank" (dhs Dietermann and Heuser Solution GmbH Greifenstein-Beilstein, Germany) recording 3 times 7 measured values, while eliminating maxima and minima values. Further, a scanning electron microscope (SEM) JEOL JSM-IT100 (JEOL Germany GmbH, Freising, Germany; magnification 1000x, acceleration voltage 10 kV, backscatter detector, low vacuum mode) and the software ImageJ (National Institutes of Health, USA; in the analyzed areas using Despeckle filter, normalization and finally Trainable Weka Segmentation tool) were used for examining the content of porosity / oxidation / cracks in the coating at three different areas of each specimen. Furthermore, SEM was also used to analyze the morphology of the coatings at different

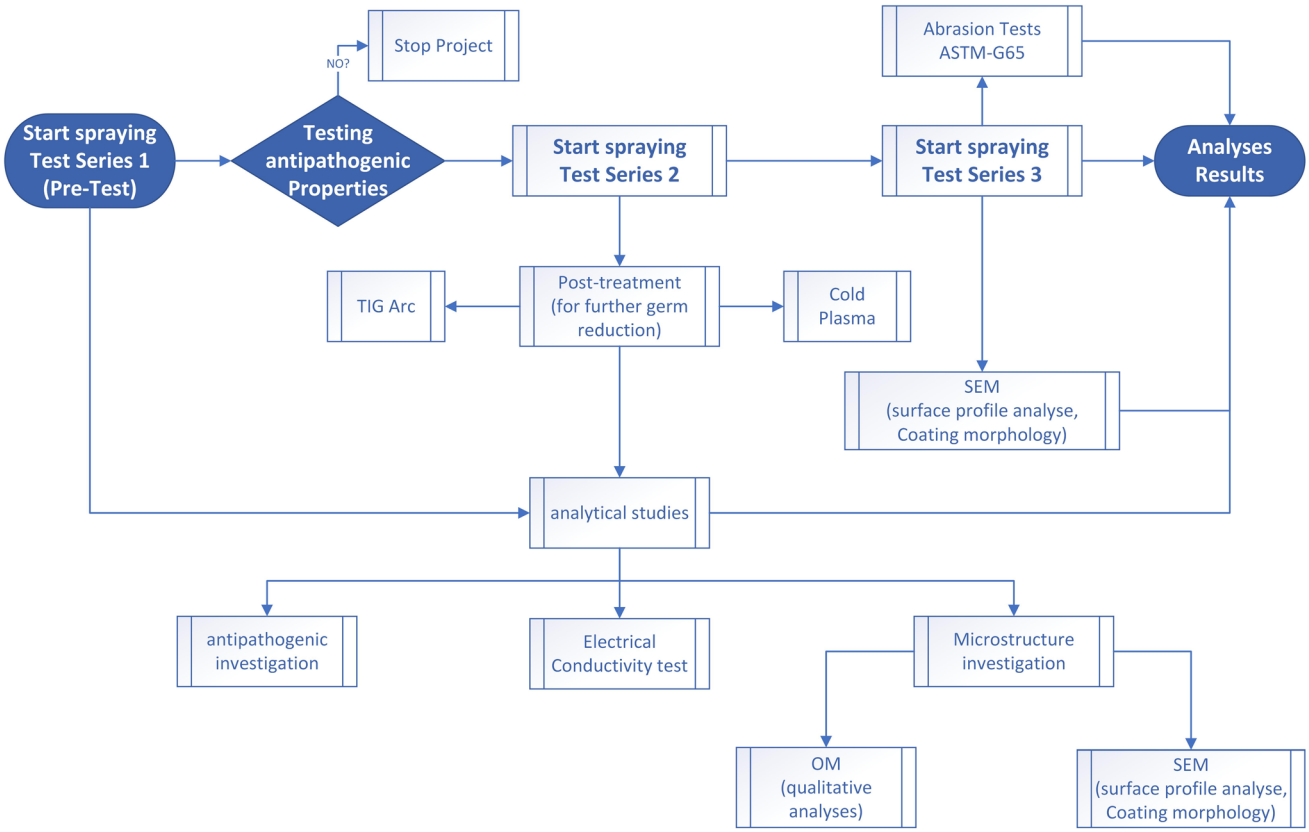

Fig. 1 Flowchart overview of test execution

Table 1 Test series 1. Overview and coating thickness

Spec. number	V1.1	V1.1P	V1.2	V1.2P
Posttreatment	…	Micro plasma	…	Micro plasma
Coating torch	Shark 1000			
Thickness, µm	29.7 ± 12.4		34.4 ± 11.0	
Gas pressure in bar/type	3.2/compressed air		3.2/N_2 + 2% H_2	

Table 2 Test series 2. Overview and coating thickness

Spec. number	V2.1P	V2.2	V2.3P	V2.4
Posttreatment	Cold plasma	…	Cold plasma	…
Coating torch	Shark400HV		Shark400RE	
Thickness, µm	148.4 ± 10.3	158.2 ± 16.2	87.3 ± 13.3	100.1 ± 8.8
Gas pressure in bar/type	3.4/Compressed air		4.0/Compressed air	
DE, %	73.8 ± 1.1	72.2 ± 1.4	62.5 ± 0.9	62.5 ± 1.0

magnifications (1000x and 3000x). With the help of SEM, the coating surface was examined, stereoscopic images were created, and surface profiles were recorded and compared. In addition, energy dispersive x-ray spectrometry (EDX) was performed in the cross-sections at the same three locations of the coatings using a JEOL Dry SD25 detector (JEOL Germany GmbH, Freising, Germany; accelerating voltage 15 kV, high vacuum mode, magnification 2000x). This made it possible to compare the determined local chemical composition of the coating surface with the morphology analysis. The EDX examinations were only carried out on the surface in order to detect any contamination caused by the posttreatment process and to show a comparison between the untreated and posttreatment sample surfaces. For qualitative analyzes, Klemm II color etchant (stock solution: sodium thiosulfate in water; etching solution: potassium persulfate) was used to improve contrasts in OM images. Finally, 3D

Table 3 Test series 1 constant parameters of arc spraying experiment

Spec. number	V1.1	V1.1P	V1.2	V1.2P
Voltage, V	27		30	
Current, A	100			
Wire feed rate v_{Wire}, m/min	3.2			
Spray offset, mm	9			
Robot speed, mm/s	666			
Number of passes	1			
Stand-off distance SoD, mm	120			

Table 4 Test series 2 constant parameters of arc spraying experiment

Spec. number	V2.3P	V2.4	V2.1P	V2.2
Voltage, V	35		32	
Current, A	120			
Wire feed rate v_{Wire}, m/min	3.2		4.2	
Spray offset, mm	5		5	
Robot speed, mm/s	700			
Number of passes	2			
Stand-off distance SoD, mm	120			

analyzes of the specimen surfaces were carried out using the same SEM and software as above. A special feature of SEM allowed the stereoscopic overlay of images of the non-tilted as well as tilted surface at the same location. This enabled 3D imaging as well as measurements of the primary profile in the SEM. In order to quantify the difference between post-treated and as-sprayed surface, a pseudo-roughness was determined by calculating distances between maximum and minimum of the respective profile and a mean contour line. This was done in both transverse and longitudinal directions with identical lengths.

Electrical Conductivity

To determine the specific electrical conductivity of the coatings, the four terminal measuring method (Loresta GX MCP-T700, Mitsubishi Chemical Analytech Co, LTD Kanagawa, Japan) was used. The measurements were carried out at two measuring points per coated substrate. Seven values were recorded for each measurement. To calculate the specific resistivity, it is necessary to convert the determined ohm resistivity. Therefore, the correction factor RCF (depending on the geometry and measuring position) and the corresponding coating thickness must be considered. For each sample the corresponding RCF was determined individually. For determining the optimum measurement range and current for the described procedure above, a computer routine was used (Ref 20). In the next step, seven characteristic resistance values were determined in the specified measuring range. This enabled more accurate measurements. For reducing the impact of leakage current and external influences on the results, the insulating base resident Table MCO-ST03 (Mitsubishi Chemical Analytech Co. LTD, Kanagawa, Japan) was used. The test method provided the electrical properties in as-sprayed and as polished states. This test method was used to be able to make a statement about the quality of the thermally sprayed coating.

Antipathogenic Research

The bacteria's used in this study were Gram-negative *Escherichia coli* (ATCC25922), Gram-positive *Enterococcus cecorum* (ATCC 43198) and Gram-positive *Staphylococcus aureus* (ATCC 25923). The first one is located in the human intestine and on mucous membranes, while the latter typically occurs in broilers farming. Bacteria from the frozen stock culture were transferred to Columbia Agar with 5% sheep blood plate and incubated at 37 °C for 18-24 h. One single colony was picked, suspended in 8 ml of sterile Tryptic Soy Broth (TSB) medium (*E.coli, E.cecorum*) or 8 ml Brain Heart Infusion (BHI) medium (*S.aureus*) and incubated over night at 37 °C. Prior to inoculation, strains were diluted with fresh TSB or BHI at 1:20. Pieces of antibacterial surfaces were placed in sterile 24 well plates—one per plate. The size of every piece was approximately 10 × 10 × 8 mm. 1.5 ml of the bacterial inoculum was pipetted into each well, followed by an incubation for 2 h (*E.coli*), 5 h (*E.cecorum*) and 4 h (*S.aureus*) at 37 °C. All samples were completely covered with the medium. Then, the supernatant was collected, and tenfold serial dilutions were made in PBS. 25 µl of serial dilutions were cultured on TSB or BHI agar plates for 18 h at 37 °C. The number of colonies per plate was recorded and used to determine the number of colonies forming units (CFU) per ml.

Posttreatment

Three different arc processes were used for posttreatment of the thermally sprayed copper coatings. The samples of test series 1 were posttreated by TIG arc and micro plasma. The posttreatment by TIG arc, Squarearc 5006 (Jäckle & Ess System GmbH, Bad Waldsee, DEU) was not successful. The high energy input from the TIG arc led to mixing of the coating with the base material. Hence, alloying elements were detected in the coating in the subsequent SEM analyzes. Furthermore, the contact between the tungsten electrode and the sample caused tungsten inclusions. Subsequently, the posttreatment by micro plasma

Table 5 Parameters for posttreatment by cold plasma

Frequency, Hz	Voltage, V	Plasma cycle time (PCT), %	Stand-off distance, mm	Number of passes	Velocity of the sample, mm/s	Plasma chamber pressure in bar
20	290	65	18	4	60	4

was focused to increase the surface energy. Since the energy input was significantly lower here, this posttreatment method led to more promising results. Posttreatment using micro plasma was carried out manually at 4.8 A with argon as the process gas. The L-TEC MIKROPLASMA 15 (L-ETC DEUTSCHLAND GmbH, Koettinger Weg 118 D.57537 Wissen, DEU) was used for the procedure. The difference to posttreatment by TIG arc consists not only in the lower arc power, moreover in the constriction of the arc. In addition to the shielding gas used in TIG welding, a plasma gas (argon) is used here, to constrict the arc in combination with a special nozzle geometry. This results in the following advantages compared to posttreatment using a TIG arc: higher arc stability, precisely adjustable penetration depth and more reliable and contactless arc ignition.

The third posttreatment for the second test series was performed with cold plasma by Openair Plasma (Plasmatreat GmbH, Birkenfeld DEU). This was used to activate the surface of the coatings. Activation of the surface means the removal or chemical conversion of inactive substances from the substrate surface by the cold plasma. Oxygen plasma was used for the activation process. The parameters for the plasma treatment are listed in Table 5. Additionally, another posttreatment method using plastic blasting abrasive MHG Kunststoffstrahlmittel Typ 2 (MHG Strahlmittel GmbH, Düsseldorf, DEU) was performed upon the coated surface, to introduce residual compressive stresses and increase the wear resistance of the coatings.

Abrasion Tests

To investigate the abrasion behavior of the copper coatings, a wear test according to ASTM G65 was carried out in addition to the antipathogenic tests. For this purpose, a new test series hereby, named as series 3 were produced and examined using the same parameters as sample V2.2 form the test series 2. The only difference to test series 2 is the variation of the coating thicknesses, because different procedures of the rubber wheel test were examined. This test series covers laboratory procedures for investigating the resistance of metallic materials to scratching abrasion by using the dry sand/rubber wheel test. The aim is to produce data that will reproducibly rank materials under a specified set of conditions. The three selected test methods include recommended procedures in the standard, which are suitable for certain degrees of wear resistance or thicknesses of the test material. These shall now be explained shortly.

Table 6 Overview of test series 3 Abrasion test according to ASTM G65 for different coating thicknesses as-sprayed and post-treated samples

Sample	Coating thickness	Posttreatment
3.1 AS	250	As-sprayed
3.2 AS	250	As-sprayed
3.3 AS	400	As-sprayed
3.4 AS	400	As-sprayed
3.1 SB	205	Sand blasted
3.2 SB	205	Sand blasted
3.3 SB	244	Sand blasted
3.4 SB	244	Sand blasted

Procedure A is the basic variant, which is used for materials on a wide scale from low to extreme abrasion resistance. All the variants tested in this work are based on it. *Procedure B* is the short-term variation of Procedure A, which has relatively severe test conditions. It is particularly useful in the ranking of medium- and low-abrasion resistant materials but can be used on highly resistant materials too. Procedure B should be used when the volume–loss values developed by Procedure A exceeds 100 mm^3.

Procedure C is the short-term variation of Procedure A for use on thin coatings.

Procedure E is the short-term variation of Procedure B that is useful in the ranking of materials with medium- or low-abrasion resistance (Ref 17).

The scope of the investigation is shown in the following Table 6.

The Parameters of the different procedures are shown in Table 7. Each procedure was performed once per sample.

Two as-sprayed and two post-treated samples with different coating thicknesses were analyzed as part of the tests. The aim of the test was to investigate the abrasion behavior of the post-treated/sandblasted samples (3.1 SB-3.4 SB) in comparison with the untreated samples (3.1 AS-3.4 AS). A better wear-resistant coating counteracts damage caused by animal beaks and thus guarantees the longevity of the component or comparison of the samples regarding the abrasion wear, scanning electron microscopy investigation was carried out for selected samples (conditions and equipment see "Microstructure section").

Table 7 Parameter of different abrasion test procedures

Specified procedure	Force against specimen, N, lb	Wheel rotation, rpm	Duration, min	Sandflow, g/min	Diameter wheel, m	Hardness rubber, A
B	130	200	10	370	0.716	60
C	130	200	0.5	370	0.716	60
E	130	200	5	370	0.716	60

Results

Direct Coating Characterization

Figure 2 gives an overview of the thermally sprayed coatings.

The color difference in coatings of different series can be explained by the fact that two different process gases were used for the test series (as already mentioned in the methods section). As nitrogen prevents the oxidation of the particles during the process, unlike compressed air, the coating in test series V2 appears significantly brighter. It can be concluded that sample coated using nitrogen as process gas (V1.2) has the most regular surface overall, probably due to low oxidation. When comparing the two configurations above, the coatings V2.3 and V2.4 sprayed with the high-speed burner have a more homogeneous surface. This is achieved by the higher particle velocity which is accomplished by the design of the torch. As a result, denser and therefore, less porous coatings can be achieved compared to conventional arc wire spraying torches. This also shows the determined standard deviation in the microscopic coating thickness measurement. A more precise adjustment in the arc spraying process was hardly possible due to the ignition characteristic of the copper wire. This had a particularly strong effect on the chosen voltage parameter. Additionally, the coatings produced with the Shark 400 RE in test series 2 show a higher DE than the coatings produced with the Shark400HV in test series 1. Since not only the application rate was highest here, but also the standard deviation was lower than for Shark 400HV.

Representative Investigation of Coating Microstructures

In essence, all coatings show a lamellar structure and are well bonded to the substrate. Figure 3 and 4 shows a comparison of cross-sections of the SEM uptake of the two investigated test series. The microstructures primarily show up in light brown tones, which can be identified as main copper α-phase (fcc). In case of samples V2.1 and V2.2, some non-melted particles can be seen. In comparison between two test series, the difference in coating characteristics due to the use of different atomizing gases is noticeable. Use of nitrogen as atomizing gas obviously leads to fewer and smaller oxides. For sample V1.1, some porosity and partial non-uniform oxidation can be seen, see detail of Fig. 3. In addition, there are some very bright areas in the OM image. Because of the change in process gas, V1.2 is less oxidized. Furthermore, darker areas with increased temperature influence form the coating process are recognizable in the surface structure. The described characteristics are confirmed by the EDX spectra of the surfaces, the results of which are summarized in Fig. 5. Thus, the bright areas for V1.1 are more likely to be impurities, mainly comprised of Al, S, C, Si and Ca. As a result of the high energy input from the micro plasma arc and the contact of the tungsten electrode with the substrate during posttreatment, impurities were detected in subsequent EDX investigations. A copper content of 90% was detected in the untreated sample V1.1. However, the copper content of the post-treated sample V1.1P was more than 95%. Furthermore, very few impurities of carbon, oxygen and partly tungsten and potassium could be detected. In contrast, no mixing of coatings could be detected in sample V1.2. The copper content here, was also about 95%. It was shown that the copper content in the thermally sprayed coating could be increased by using nitrogen as a process gas. However, the measured content of element also depends on measurement methods. In this work solely EDX was used to determine the copper content. EDX is not as exact as OES. Therefore, the comparison between the samples is to be assessed rather qualitatively. Nevertheless, burn-off as a result of the process was detectable. Furthermore, no tungsten and potassium contamination could be detected here. For the posttreatment of the samples by arc, two different approaches were investigated.

Figure 6 shows the differences in the surface characteristics of the first investigated test series. In the comparison of samples V1.1 without posttreatment and V1.2 with posttreatment, it is noticeable that the pseudo-roughness of the untreated variant is somewhat higher or equal, compare Table 8. The size of the specific surface, on the other hand, is larger in the post-treated variant. This can be seen clearly by looking at the primary profiles in Fig. 6, where a large number of finely distributed and more frequent peaks are found. In general, a finer, flatter profile is

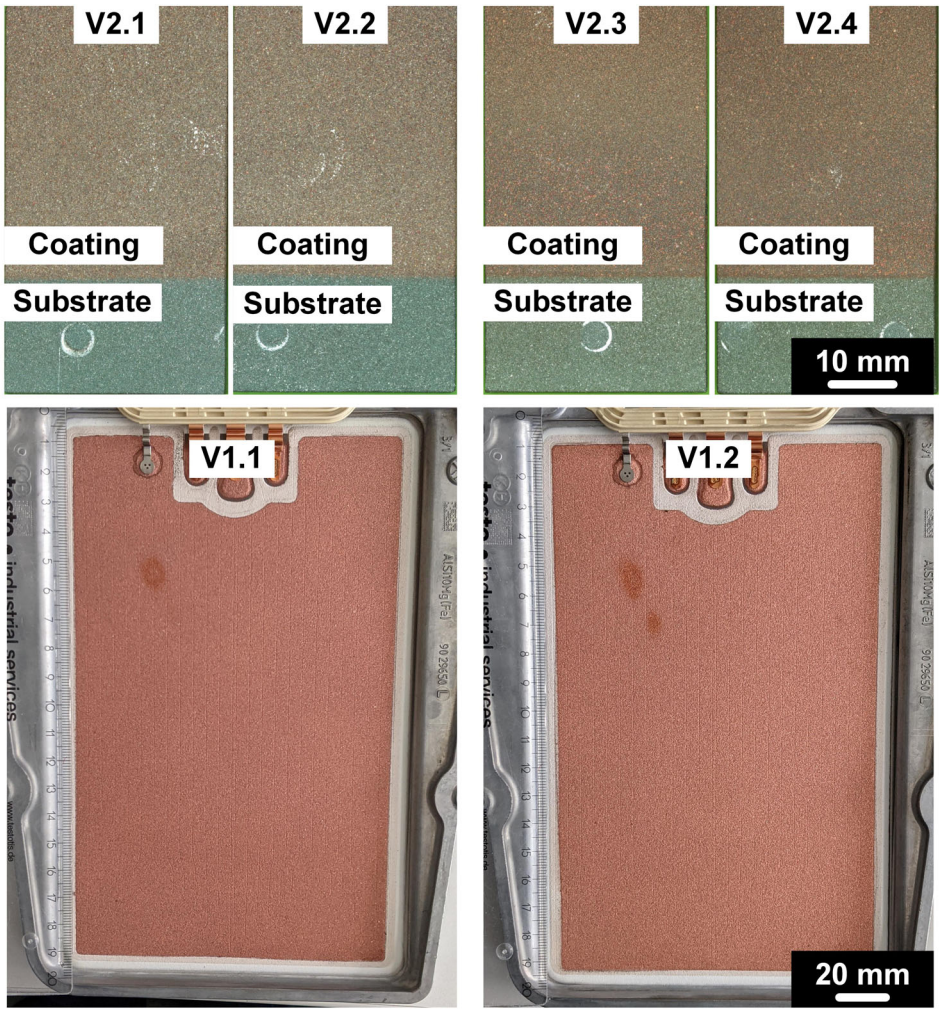

Fig. 2 Surfaces of the twin-wire arc-sprayed copper specimens of Test series 2 (top) and Test series 1 (bottom)

seen here, except for some peaks. Irrespective of this, the surface structure of a thermally sprayed coating is always dependent on the roughness of the substrate surface.

Comparing the pseudo-roughness of test series 1, it is noticeable that the profiles of the transversal roughness are quite similar. The same can be said for the longitudinal roughness profiles. The samples of test series 2 show a higher transverse and lower longitudinal roughness than the samples of test series 1. This could be related to the variation of the process gas. However, there is also large anisotropy between the longitudinal and transverse direction noticeable.

Quantitative Coating Analyzes and Electrical Properties

In Table 9, the electrical conductivity of the coatings is displayed next to the sum of coating defects. To determine the defect density, the image processing software ImageJ was used as described in the experimental methods section (3 images). The trainable WEKA plugin uses a machine learning algorithm and thus is adaptable to the specific coating (custom data and identifiers).

The results show a direct correlation between electrical conductivity and coating defect. Since the coatings were applied to two different base materials in each test series, the determined coating thicknesses were used as reference values for measuring the electrical conductivity. The measured conductivities differ for test series 1 and 2. The samples sprayed with the high-speed torch had the highest electrical conductivity, while this was significantly lower for the samples of the test series 1. The samples V2.1P and V2.2, which were sprayed with the Shark 400 RE, showed the highest coating defect density. Due to the different geometries of the substrates, the results of the electrical conductivity investigations are rather qualitatively comparable. Based on the investigations, it can be said that the electrical conductivity can be used to make a statement about defect density and thus about the quality of the thermally sprayed coating (Ref 21).

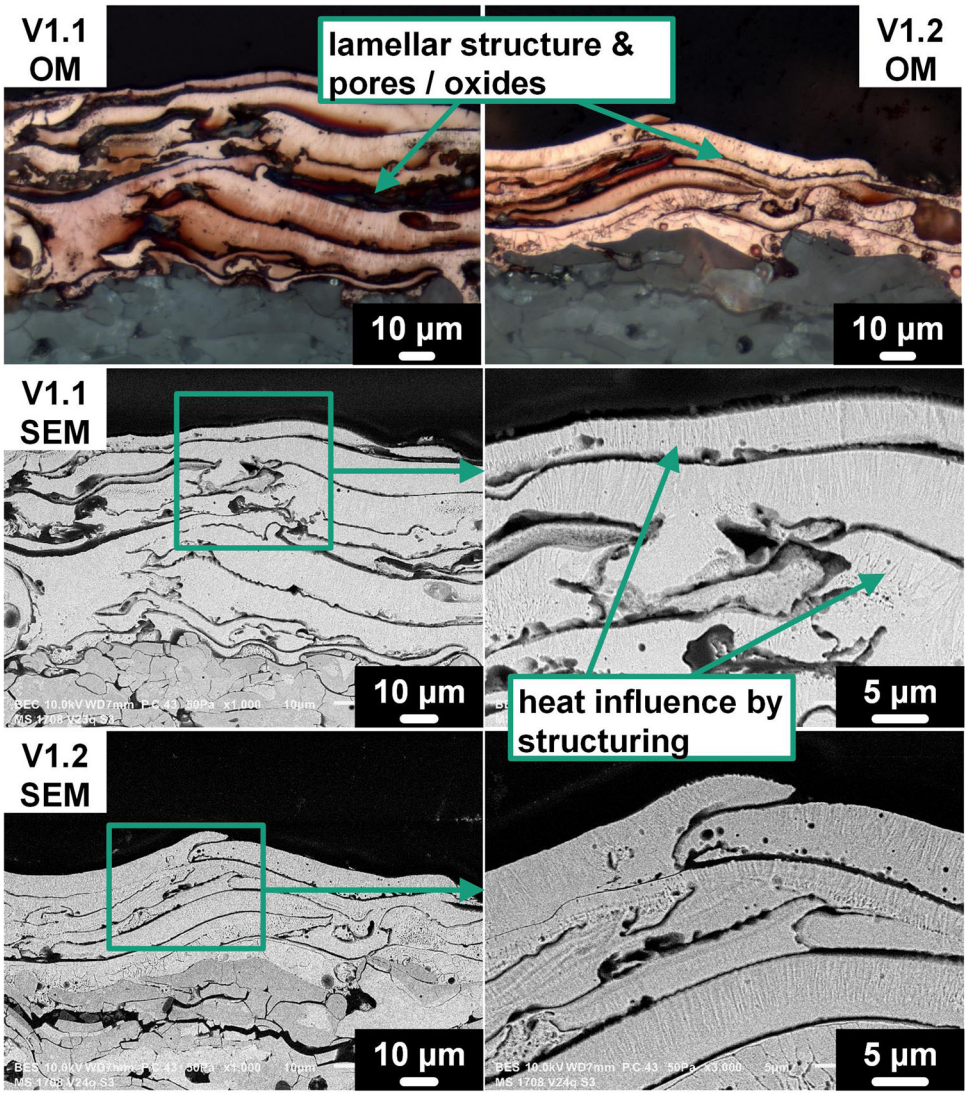

Fig. 3 Representative morphology of Test series 1 by OM (top) and SEM (bottom) as an overview and by SEM in detail (right)

Antipathogenic Studies

The results of the antipathogenic tests are shown in Fig. 7. The ordinates of the diagrams represent the colony-forming units per milliliter, while the abscissae presents are divided according to the respective samples of Series 1 and 2. To illustrate the antipathogenic effect, an untreated reference sample (UC) made of nickel-chromium-steel was also examined in each case. Figure 7(A) and (B) demonstrates that the inhibitory effects of the coatings on *E.cecorum* is less important than the effect on *E.coli* and *S.aureus*. The plate count of *E.cecorum* after co-culture with surfaces was lower compared with untreated control (UC). The growth inhibiting activities of the coated surfaces of series 2, i.e., V2.1, V2.2, V2.3P and V2.4 were more effective compared to that of series 1, see Fig. 7(C). Thus, a comparison between both the test series shows that the samples of the second test series allowed significantly less nucleation than the samples of the first test series. Furthermore, the post-treatment with cold plasma grade contributes to a further reduction in the microbial load of the *E.coli* strain, but not for the other germs. Comparing the post-treated samples from both test series it becomes clear that posttreatment with cold plasma can further inhibit bacterial growth in some cases. However, the standard deviation has to be considered here too. When comparing the two posttreatment processes, posttreatment by means of cold plasma causes a slightly higher reduction of bacteria growth. Overall, the results indicate that all coatings have a growth inhibitory effect on *E.coli*, *S.aureus* and *E.cecorum*. Data also suggests that surfaces V2.1, V2.2, V2.3 and V2.4 have a higher inhibitory potential.

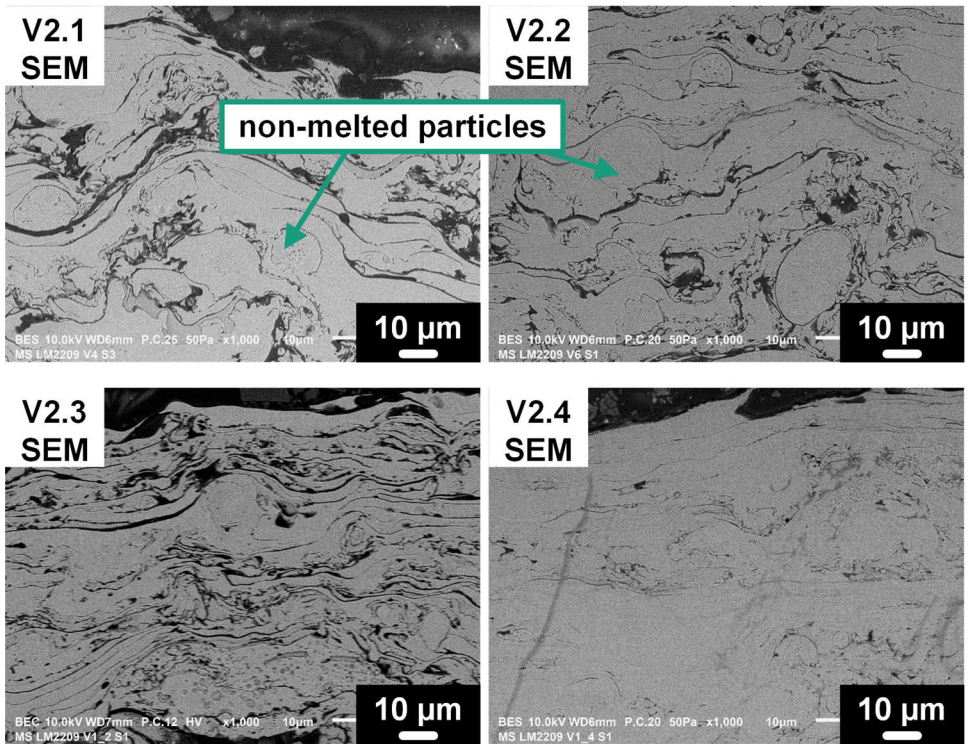

Fig. 4 Representative morphology of Test series 2 by OM (top) with and SEM (bottom) as an overview and by SEM in detail (right)

Abrasion Tests

The results of the abrasions test can be seen in Fig. 8. The diagram shows a comparison between the three selected test procedures. Each of the selected test methods represents a different load case, as it is not possible to predict which of these methods comes closest to the application. Hence, three different variants were analyzed. It is clearly visible that the post-treated samples have a higher abrasive wear resistance compared to samples without any post-treatment. This happens because the mass loss is significantly lower for procedure B and E. Only test method C shows approximately similar mass losses for both kind of samples with a test duration of 30 s. In general, the test force was the same for all three test methods, while the test duration was varied.

In order to visualize the abrasion wear and to compare the surfaces of the two specimens, SEM examinations were then carried out and are shown in Fig. 9. The figure shows a comparison between the samples with and without post-treatment. The results show a more compact surface for the sandblasted sample before testing. In general, the erosion on both samples is very homogeneous. When comparing the abrasion results, it is noticeable that the wear marks are more clearly visible in the samples that have not been post-treated.

Discussion

The aim of this study was to investigate coatings with respect to their antipathogenic properties. At the same time, however, the application of the coatings is linked to other properties, some of which have not yet been considered at all or only to a limited extent such as the abrasion resistance or the chemical resistance. Overall, the coatings showed a regular homogenous structure with some staining in the regions exposed to stronger heat input. The microstructure was presented by correlative microscopy. The approach used showed differences in the imaging capability and in the interpretation of chemical compounds. For example, some black areas which could be interpreted as porosity by OM are more likely to be identified as complex compounds in SEM/EDX. For that reason, SEM images were evaluated for quantitative coating analysis, while a good impression in terms of quality was given by comparing SEM and OM. A very regular, mostly lamellar morphology with a moderate porosity and low oxidation content was achieved, which could be manipulated by the process parameters. Possible factors influencing the determined porosity could lie in the cross-section preparation or the non-molten / bound particles in some samples. The use of nitrogen and the shroud effect thus provided a better coating quality by effectively shielding the particles from the atmosphere for series 1. For this reason, the coating defects in sample V1.2 are significantly lower.

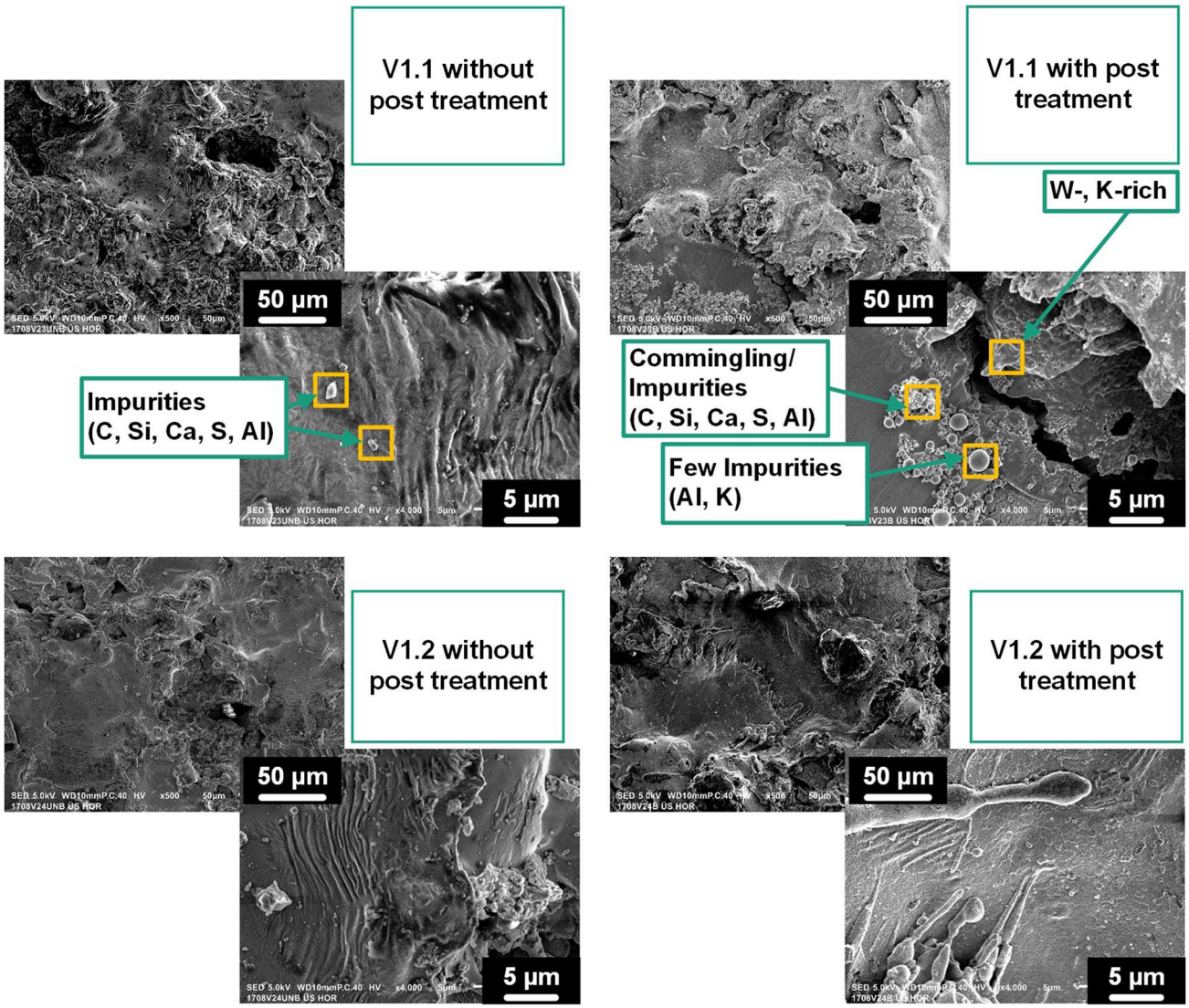

Fig. 5 Detailed surface morphology of the coatings of Series 1 by SEM. The regions highlighted with yellow boxes show the locations, where EDX analysis was performed to obtain the composition spectrums and detect the local differences in composition and presence of impurities/defects

Furthermore, the coatings attained with the use of a high velocity torch showed lower coating defects.

Correlating the values of defect content and electrical conductivity in Table 9, different trends become apparent. Comparing the samples produced with the same type of torch (V1.1 versus V1.2; V2.1P versus V2.2; V2.3 versus V2.4) it is noticeable that an increased content of pores and oxides correlates with a lower conductivity i.e., higher resistivity. The different conductivities between the test series mainly arise due to the different geometry of substrate, coating thickness, substrate material of the respective samples and the variation of the process gas. While at the beginning of the investigations, preliminary tests were mainly carried out on test sheets from other projects, the selection in the second series of tests was concretized on substrates intended for this purpose. Considering the second test series, it is noticeable that the defects in coatings attained using the high velocity torch are much lower. Due to the higher particle velocities of the torch, the spray particles have lesser time to interact with the atmosphere. Furthermore, a higher electrical conductivity can also be observed here. In contrast, the conventionally arc-sprayed coatings have a slightly lower conductivity and a slightly higher defect density. In conclusion, it could be shown that a higher defect level leads to a lower electrical conductivity.

Another outcome of this investigation is that the thermally sprayed copper coatings can significantly limit the growth of antipathogenic germs. The bacterial load of the first two bacterial strains *E. coli* and *S. aureus* are mainly

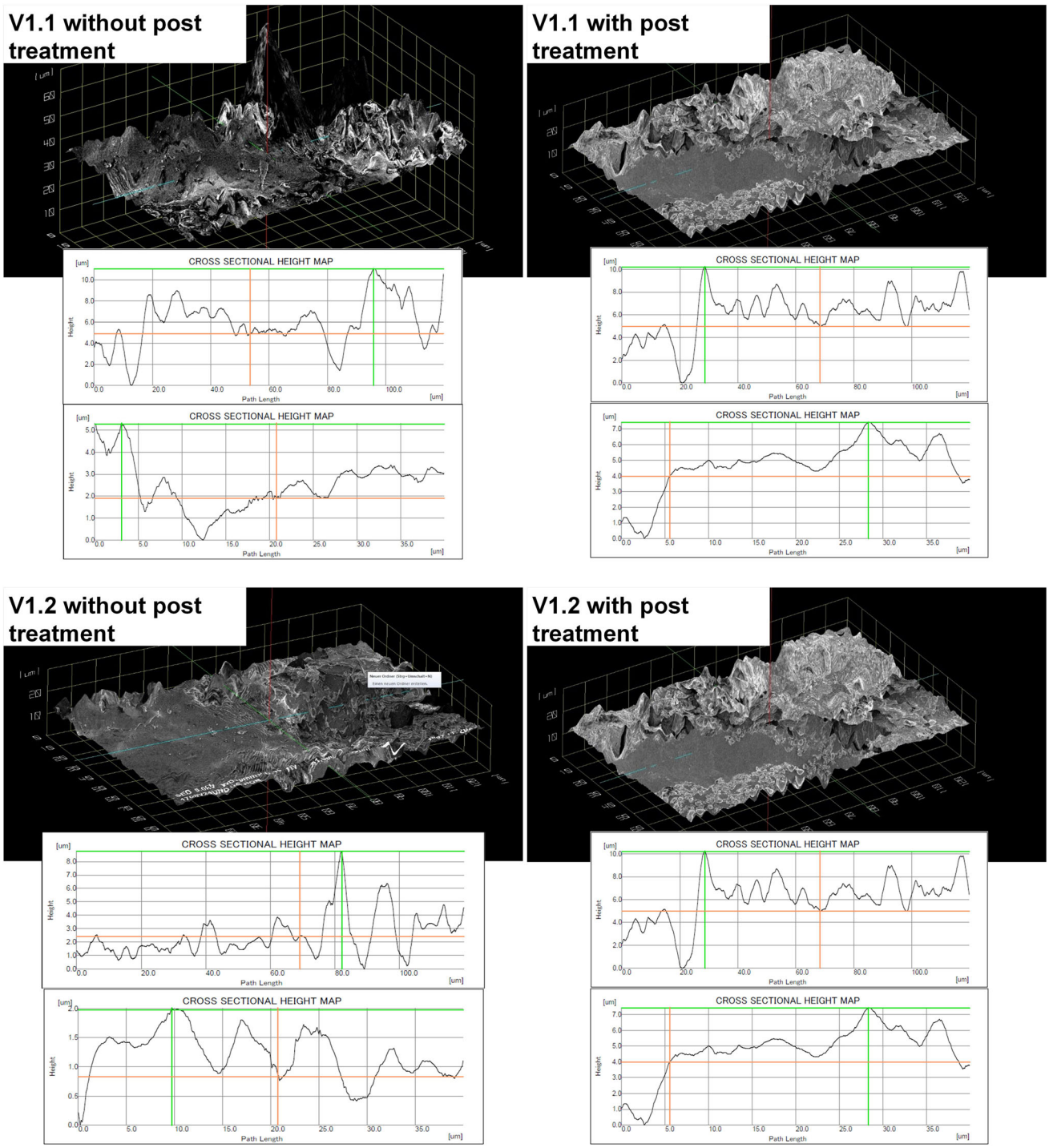

Fig. 6 Surface profiles of specimens of Series 1 (top). Comparison of the pseudo-roughness in transverse (middle) and longitudinal direction (bottom)

found in the human beings, while the third is found specifically in the field of broiler farming. Furthermore, it was found that although non-destructive coating characterization by electrical conductivity is possible, it may not necessarily provide information about the anti-infective property of the coating. However, it made sense to carry out this investigation to prove the correlation between defect density and electrical conductivity. It could be shown that the choice of the high velocity torch can reduce the defect density of the thermally sprayed coating. Long-term tests will show whether the antipathogenic effect of

Table 8 Comparison pseudo-roughness of test series 1 path length-transversal 120 µm, longitudinal 40 µm

Samples	V1.1 without posttreatment	V1.1 with posttreatment	V1.2 without posttreatment	V1.2 with posttreatment
Transversal	6.14	5.23	6.36	8.13
Longitudinal	3.36	3.43	1.14	1.06

Table 9 Sum of defects (Porosity/cracks/oxide) and electrical conductivity of the coatings

Spec. number	Defects (Porosity/cracks/oxides), %	Electrical conductivity, 10^6 S/m
V1.1	8.57 ± 2.65	8.04 ± 3.10
V1.2	5.02 ± 1.98	9.87 ± 5.25
V2.1P	10.88 ± 1.41	23.5 ± 0.08
V2.2	12.52 ± 3.92	20.7 ± 0.10
V2.3P	10.03 ± 1.23	28.9 ± 0.14
V2.4	5.94 ± 2.31	29.3 ± 0.13

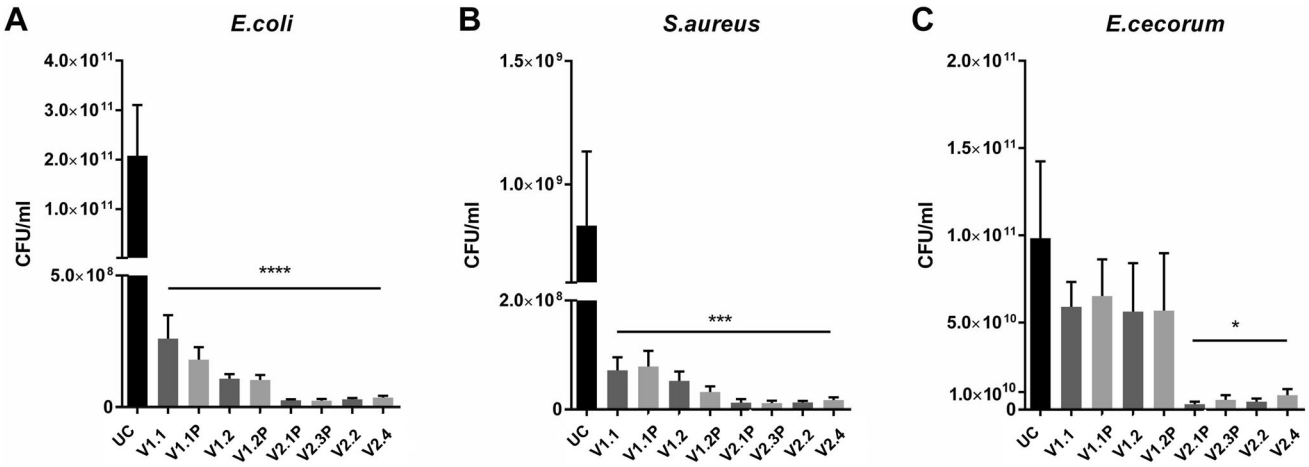

Fig. 7 In vitro growth inhibitory effect against E.coli (A), S.aureus (B) and E.cecorum (C). Viable bacteria were quantified in the medium after 2 h (E.coli), 4 h (S.aureus) and 5 h (E.cecorum) of cultivation with and without coatings Data is presented as sum of mean ± standard deviation ($n = 5$ (E.coli); $n = 4$ (S.aureus); $n = 6$ (E.cecorum)). $^*p < 0.05$, $^{***}p < 0.001$, $^{****}p < 0.00001$ vs. untreated control (UC)

the copper coating will be permanent. However, it has been shown that copper coatings are biocidal here.

The abrasion tests have revealed that sandblasting is a suitable posttreatment method to increase the wear resistance of thermally sprayed coatings. Previously carried out studies show that, shot peening as a posttreatment has considerable effect on improving wear resistance of thermal spray coatings (Ref 18). Within the scope of this project, a posttreatment using spherulitic blasting material is carried out. However, the focus here is on increasing the abrasion resistance of thermally sprayed coatings (Ref 15, 19). The detailed images obtained through the scanning electron microscope show that the plastic blasting agent contributed to a compression of the thermally sprayed coating. Probably due to residual stress introduced through blasting, a comparatively higher resistance to abrasion wear could be demonstrated in the abrasion test.

Additionally, the mentioned posttreatment methods showed additional germ reduction in some samples. A possible cause for this could be the reduction of bacterial adhesion as described in Ref 15 by plasma treatment. For example, in medicine, plasma treatment under atomic pressure (CAP) is used to generate active radicals for in situ treatment. These have a bactericidal effect. In this context, it was found that posttreatment with micro plasma is significantly more suitable than posttreatment with TIG. Furthermore, surface activation by means of cold plasma in the second series of experiments also led to a reduction in bacterial growth.

It is yet to be investigated whether possible aging effects play a role since samples V1.1 and V1.2 are significantly

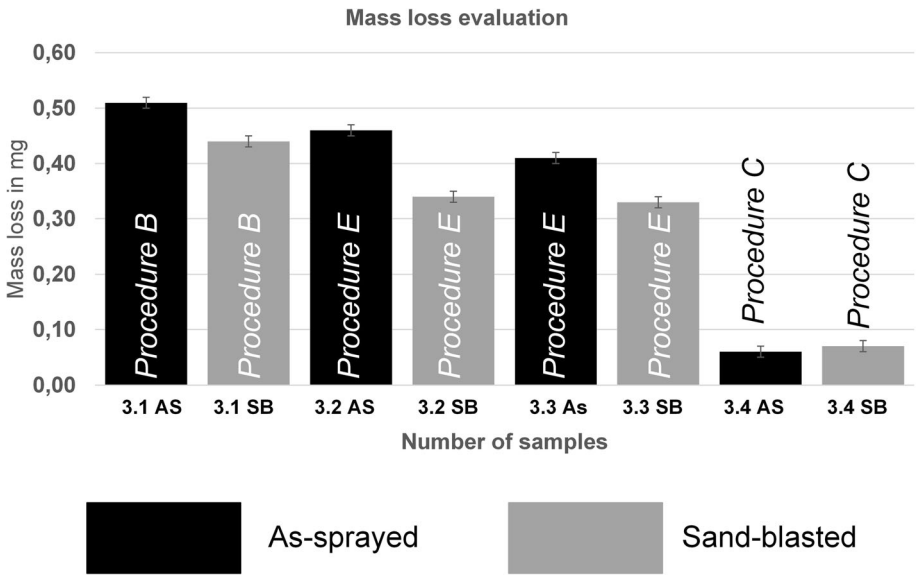

Fig. 8 Abrasion test results by rubber wheel test ATSM- G65. Comparison between different test procedures for as-sprayed samples without any posttreatment and samples with posttreatment using plastic blasting agents for test series 3

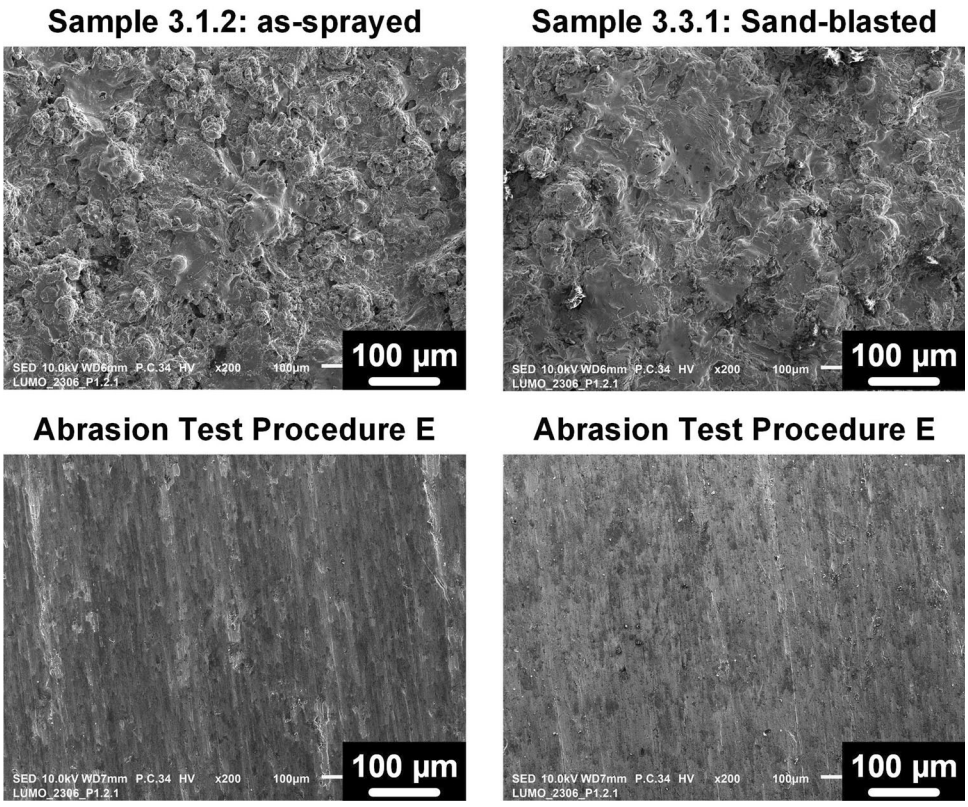

Fig. 9 Comparison of surface texture of test series 3 after abrasion test for as-sprayed samples without any posttreatment (left) and post-treated samples (right)

older than the other thermally sprayed coatings or whether the selection of the torch type in combination with the parameter variation caused an enhancement of the anti-pathogenic effect.

Finally, the investigations carried out showed that the thermally sprayed copper layers in this research project could contribute to a significant reduction in bacterial growth and thus offer the potential to contribute to a reduction in the use of antibiotics in fattening livestock.

Summary and Outlook

In this work, 99% copper alloy wire was sprayed using twin-wire arc spray process for application in anti-pathogenic environments. Compressed air and nitrogen were used as process gases. Additionally, the type of torch and the post-processing were varied. Promising coating properties were achieved, especially for germs occurring in broiler farming. Furthermore, posttreatments with micro

plasma show the possibility of further reducing the growth of germs. Thus, the spread of antibiotics-resistant germs can be reduced in the long term to sustainably protect the health of animals and humans. To increase the wear resistance of the copper coatings, sandblasting as a post-treatment method was investigated and tested. Further focus will be the investigations regarding ammonia resistance and the long-term effect of the antipathogenic coating properties.

Conclusion

The aim of this work was to demonstrate the antipathogenic properties of thermally sprayed copper coatings with regard to a specific application that is broiler farming. As part of the project, it was demonstrated that copper coatings significantly inhibit the growth of the bacteria tested in comparison with nickel-chromium-steel. The winner of the test series was sample V2.3, which was able to further reduce bacterial growth in direct comparison to sample V2.4 for all three typical bacterial strains through posttreatment using cold plasma. Furthermore, the abrasion resistance of the coatings was analyzed and improved due to the field of application, as these coatings will be in direct contact with the animals. On the one hand, wear tests proved that shot peening improves resistance to abrasion. Additionally, scanning electron microscopy has shown that the surface is compacted by the posttreatment process, and is therefore, more resistant. To be able to use the coating in fattening operations, the ammonia resistance must be investigated and increased in the further course of the project, as the concentration is significantly high in this environment.

Funding Open Access funding enabled and organized by Projekt DEAL.

References

1. M. Razavipour, N. Singh, B. Jodoin, M. Gonzalez, and E. Alarcon, J. Villafuerte, Enhanced Antibacterial Properties of Copper Surfaces Using Cold Spray Shot Peening, in *Proceedings ITSC 2021*, (Indianapolis, USA, 2021), pp. 268-273
2. H.T. Michels, S.A. Wilks, J.O. Noyce, and C.W. Keevil, Copper Alloys for Human Infectious Disease Control, in *Materials Science and Technology Conference*, (Pittsburgh, USA, 2005)
3. T. Van Limbergen, S. Sarrazin, I. Chantziaras, J. Dewulf, and R. Ducatelle, Risk Factors for Poor Health and Performance in European Broiler Production Systems, in *BMC Veterinary Research*, (Gent, NLD, 2019)
4. BMJ, *Bekanntmachung zur Förderung von Maßnahmen in der Geflügelhaltung, die zur Reduktion des Auftretens von Infektionserkrankungen und der Notwendigkeit zur Behandlung mit antibiotischen Tierarzneimitteln beitragen*, (Berlin, DEU, 2021)
5. H.T. Michels and C.A. Michels, Can Copper Help Fight COVID 19?, *Adv. Mater. Process.*, 2020, **178**, p 21-25.
6. P. Bleichert, C. Espírito Santo, M. Hanczaruk, H. Meyer, and G. Grass, Inactivation of Bacterial and Viral Biothreat Agents on Metallic Copper Surfaces, *Bio Metals*, 2014, **27**, p 1179-1189.
7. D. Mitra, E.T. Kang, and K.G. Neoh, Antimicrobial Copper-Based Materials and Coatings: Potential Multifaceted Biomedical Applications, *ACS Appl. Mater. Interfaces*, 2019, **12**(19), p 21159-21182.
8. J. Mostaghimi, L. Pershin, H. Salimijazi, M. Nejad, and M. Ringuette, Thermal Spray Copper Alloy Coatings as Potent Biocidal and Virucidal Surfaces, *J. Therm. Spray Tech.*, 2021, **30**, p 25-39.
9. N. Bharadishetta, K.U. Bhat, and D. Bhat Panemangalore, Coating Technologies for Copper Based Antimicrobial Active Surfaces: A Perspective Review, *Metals*, 2021, **11**, p 711.
10. M. Rosenberg, K. Ilić, K. Juganson, A. Ivask, M. Ahonen, I.V. Vrček, and A. Kahru, Potential Ecotoxicological Effects of Antimicrobial Surface Coatings: A Literature Survey Backed up by Analysis of Market Reports, *PeerJ*, 2019, **7**, e6315.
11. G. Grass, C. Rensing, and M. Solioz, Metallic Copper as an Antimicrobial Surface, *Appl. Environ. Microbiol.*, 2010, **77**(5), p 1541-1547.
12. G. Borkow and J. Gabbay, Copper, an Ancient Remedy Returningto Fight Microbial, Fungal and Viral Infections, *Curr. Chem. Biol.*, 2009, **3**(3), p 272-278.
13. V. Champagne, K. Sundberg, and D. Helfritch, Kinetically Deposited Copper Antimicrobial Surfaces, *Coatings*, 2019, **9**(4), p 257.
14. V. Gorokhovsky and P. Belluz, Ion Treatment by Low Pressure Arc Plasma Immersion Surface Engineering Processes. Surface & Coatings Technology, *Surf. Coat. Technol.*, 2013, **215**, p 431-439.
15. M. Baleani, M. Viceconti, and A. Toni, The Effect of Sandblasting Treatment on Endurance Properties of Titanium Alloy Hip Prostheses, *Artif. Organs*, 2001, **24**(4), p 296-299.
16. F.L. Tabares and I. Junkar, Cold Plasma Systems and Their Application in Surface Treatments for Medicine, *Molecules*, 2021, **26**(7), p 1903.
17. ASTM G65-16, in *Standard Test Method for Measuring Abrasion Using the Dry Sand/Rubber Wheel Apparatus*, (West Conshohocken, USA, 2021)
18. H. Mohassela, F. Malekabadib, M. Jebreilic, M. Zehsazc, and F. Vakili-Tahamic, Effect of Shot Peening on Tribological Behaviors of Molybdenum-Thermal Spray Coating Using HVOF Method, *Tribol. Ind.*, 2017, **39**(1), p 100-109.

19. A.W. Eberhardt, B.S. Kim, E.D. Rigney, G.L. Kutner, and C.R. Harte, Effects of Precoating Surface Treatment on Fatigue of Ti6Al4V, *Mater. Sci. Forum*, 2002, **404-407**, p 457-462.
20. M. Hauer et al., Highly Efficient Thermal Barrier Coatings based on Arc Spraying of Amorphous Fe-based Alloys and NiCrAlY for use in LH2 Tanks and Other Cryogenic Environments, *J. Therm. Spray Tech.*, 2023, **32**(1-2), p 327-338.
21. L. Pawlowski, *The Science and Engineering of Thermal Spray Coatings*, 2nd ed. Wiley, West Sussex, 2008, p 350-357